Published in final edited form as:
Comput Med Imaging Graph. 2012 January ; 36(1): 72–84. doi:10.1016/j.compmedimag.2011.06.002.

Computer-Assisted Detection of Infectious Lung Diseases: A Review

Ulas Bagci,
Center for Infectious Disease Imaging, Department of Radiology and Imaging Sciences, National Institutes of Health (NIH), Bethesda, Maryland 20892

Mike Bray,
National Institute of Allergy and Infectious Diseases, National Institutes of Health (NIH), Bethesda, Maryland 20892

Jesus Caban,
National Library of Medicine, National Institutes of Health (NIH), Bethesda, Maryland 20892

Jianhua Yao, and
Department of Radiology and Imaging Sciences, National Institutes of Health (NIH), Bethesda, Maryland 20892

Daniel J. Mollura
Center for Infectious Disease Imaging, Department of Radiology and Imaging Sciences, National Institutes of Health (NIH), Bethesda, Maryland 20892

Abstract

Respiratory tract infections are a leading cause of death and disability worldwide. Although radiology serves as a primary diagnostic method for assessing respiratory tract infections, visual analysis of chest radiographs and computed tomography (CT) scans is restricted by low specificity for causal infectious organisms and a limited capacity to assess severity and predict patient outcomes. These limitations suggest that computer-assisted detection (CAD) could make a valuable contribution to the management of respiratory tract infections by assisting in the early recognition of pulmonary parenchymal lesions, providing quantitative measures of disease severity and assessing the response to therapy. In this paper, we review the most common radiographic and CT features of respiratory tract infections, discuss the challenges of defining and measuring these disorders with CAD, and propose some strategies to address these challenges.

Keywords

Infectious Diseases; Computer Assisted Detection; Texture Analysis; Lung CT; Feature Extraction; Tomography

1. Introduction

As shown by the recent pandemic of novel swine-origin H1N1 influenza, respiratory tract infections are a leading cause of disability and death. Radiologic diagnosis using cross-

sectional and projectional imaging techniques such as chest radiography and computed tomography (CT) remains the most important modality for the first-line assessment of acutely ill patients [1]. However, radiologic assessment is significantly restricted by its low specificity, due to the similar appearance of infectious, inflammatory and some neoplastic abnormalities and the absence of validated measures of disease severity. These limitations raise the possibility that radiologists' assessment of respiratory tract infections could be enhanced through the use of computer-assisted-detection (CAD) systems. The use of CAD for quantitative measurement of pulmonary disease could also provide numerical data for correlation with fever, leukocyte counts and other quantitative laboratory variables.

CAD is increasingly being used to supplement traditional methods of evaluating malignancies, pulmonary fibrosis and other chronic medical conditions. In this article, we propose that CAD could also be used to evaluate and manage respiratory tract infections. The first section reviews common causes of infection and how their corresponding imaging findings may be productive areas for further CAD development, to generate tools for research and for patient management. After giving brief information about infectious lung diseases in Section 2, we provide an overview of CAD systems for assessing pulmonary disease and their use in clinical settings in Section 3. In Section 4, we describe the currently used image acquisition process for most CAD systems for lung diseases. In Section 5, we discuss texture extraction and classification methods for CAD systems in pulmonary infections. In Section 6, we first explain performance evaluation criteria for CAD systems in general, and we then explain qualitative and quantitative measures to evaluate the extent of infection. The final section discusses the limitations of current CAD systems for respiratory tract infections and some possible strategies for future development.

2. Respiratory tract infections

Respiratory tract infections caused by viruses, bacteria, fungi and parasites are a major component of global infectious disease mortality. CT examination of the lungs during acute respiratory tract infections has become an important part of patient care, both at diagnosis and monitoring progression or response to therapy. Common CT findings associated with respiratory tract infections include ground-glass opacity, tree-in-bud nodularity, random distribution of nodules, linear interstitial/bronchovascular thickening, and consolidations [1]. Although none of these visual patterns is specific for one pathogen, the amount of lung volume exhibiting these features can provide insights into the extent or severity of infection. For example, tree-in-bud nodularity is associated with inflammation of the small airways (bronchioles), such as in viral or bacterial bronchiolitis, and the increasing sizes of abnormal regions on CT can signal the progression of infection. Ground-glass opacity, in which there is partial filling of interstitial and alveolar structures with infectious and inflammatory material, is a very common abnormality associated with numerous infections [48]. The transition in patterns over time, such as tree-in-bud opacity changing to ground glass opacities (GGO) and eventual consolidation, can also provide insight into the progression of pulmonary disease.

Historically, radiologists have interpreted these findings subjectively, by visually estimating the extent of lung parenchyma having abnormal visual features, and published research has employed semi-quantitative measurement scores based on visual analysis. CAD provides the opportunity to use systematic methods for measuring lung volumes manifesting particular imaging patterns as a first step. Then, CAD increases sensitivity, specificity, and precision of measurements in correlating radiographic features with underlying pathology and clinical variables [2].

3. CAD systems in Medical Imaging

Significant progress in image acquisition technologies such as positron emission tomography (PET), magnetic resonance imaging (MRI) and CT is making it possible for image analysis to be used in CAD systems and for planning surgery, radiation treatment and other types of therapy. The uses of these technologies to detect, understand, diagnose and treat disease are areas of active research from which new CAD systems can be developed. CAD is an intensive tool that provides radiologists with a “second opinion” to improve the sensitivity and specificity of their diagnostic decision-making [3]. Although the ultimate aim of CAD systems is to provide diagnostic information to improve clinical decision-making, its success depends principally on disease detection [4].

CAD systems are widely used to detect and diagnose numerous abnormalities in routine clinical work. They are usually specialized for anatomical regions such as the chest, breast or colon, and for certain imaging technologies such as radiography, CT or MRI [5]. Applications of CAD systems include the detection of clustered micro-calcifications in mammograms, intracranial aneurysms in magnetic resonance angiography (MRA) and interval changes in successive whole-body bone scans [3].

The development of a new CAD system typically begins with the identification of a clinically important problem. The problem is then analyzed using imaging and clinical findings, based on human recognition of normal and abnormal features. Radiologists’ visual interpretations, combined with physicians’ clinical data analysis, contribute significantly to understanding clinical needs at this step. Third, the imaging and clinical findings are incorporated into the computational environment by means of automated or semi-automated algorithms. This step includes texture, shape and spatial analysis of observed patterns and their classifications.

In general, the medical literature distinguishes three principal applications for the computerized detection and analysis of diseases. As applied to respiratory tract infections, these are:

- Understanding: the use of imaging to identify, understand, and diagnose infectious pulmonary diseases;
- Preprocessing: Algorithms for segmentation and registration of pulmonary anatomical structures; and
- Detection and classification: the application of texture and shape analysis to image processing to develop accurate, reliable, and robust detection and classification systems for respiratory tract infections.

In this paper, we focus on the first and third applications of CAD. Because the general processing of lung images (CAD-preprocessing), including segmentation and registration in normal and diseased subjects, have been well characterized in the medical literature, we have excluded that step from this paper. Comprehensive reviews of algorithms for segmentation and registration of anatomical structures in the chest can be found elsewhere [6,7].

4. Image acquisition

Some characteristics of image acquisition that are not disease-specific, such as patient position, level of respiration, and reduced dose technique, play a significant role in the interpretation of CT and radiograph scans. Since the advent of high-resolution CT (HRCT), thin-slice CT scans with sub-millimeter resolution have become an indispensable part of chest radiology, allowing the examination of the lung parenchyma with improved contrast,

spatial resolution, and a level of detail that is only otherwise possible from biopsy or postmortem specimens [1, 6]. CT is therefore the most powerful tool for the assessment of the lung parenchyma. Density differences in normal and diseased lungs are more apparent in CT scans, and because of its higher sensitivity compared to plain-film radiography, CT imaging provides better identification, localization, and quantification of small lung nodules [8,51,52,54]. Specifically, the use of thoracic thin-section CT scans for recognition and quantification of inflammatory and infectious diseases continues to improve, as the visual quantification of the extent of disease from 2D chest radiographs is less accurate than from CT images. On the other hand, although the interpretation of radiograph scans is notoriously difficult, such that large inter-observer variability is inevitable [9], certain advantages of the chest radiograph cause it to continue to be requested as a first step in investigation [10].

5. Detecting and understanding disease processes

A significant part of the interpretation of radiographic and CT scans is the detection of characteristic abnormalities. Visual patterns associated with abnormal anatomy in medical images carry valuable information, especially when the normal anatomy and its visual (textural or shape) patterns are known. A number of studies have reported that diagnostic confidence and consistency can be improved by using image processing techniques. These methods extract textural and shape patterns from scans and apply pattern recognition methods to the extracted information to learn normal and abnormal textural and shape patterns [6, 11–16].

Commonly observed patterns, associated with abnormal lung anatomy, in chest radiographs and CT images can be divided into four groups, based on shape, texture and attenuation information (Table 1). The presence of more than one type of abnormality in the same region of interest can cause difficulty in understanding and interpreting the nature and extent of a disease. That situation is referred to as a “mixture” in Table 1.

5.1. Feature extraction

Despite extensive investigation of textural analysis techniques for the detection, classification, and quantification of disease patterns in the chest, the relationship between specific lung diseases such as influenza and their unique textural or shape patterns remains poorly characterized. This section explains computerized features pertaining to radiological findings from respiratory tract infections that can be extracted using image processing methods.

5.1.1. Low-level features—Any method of feature analysis relies on an appropriate representation of shape and/or appearance information and developing that representation for further classification [17, 18]. Based on how human beings interpret image information [19], the appearance, shape, spectral and textural, and contextual features are some fundamental feature types that have been computerized in various image-processing applications, including CAD systems. Among those feature types, representing the appearance of medical images (CT scans and radiographs in this particular case) in the most discriminatory way eases the classification procedure. Early approaches for texture classification in CAD systems of lung diseases focused on analysis of first-order or second-order statistics of textures [6], statistical and fractal texture features, ridge and numerous texture features derived from a grey level co-occurrence matrix (GLCM), and some basic shape-based features to detect nodular structures. More recent approaches have focused on spatial/frequency analysis of textures, wavelets, Gabor filters, local binary signatures and high-level features, providing good multi-resolution analytical tools for texture analysis and classification with promising experimental results [20–26].

5.1.2. High-level features—High-level features significantly affect the way objects are recognized and understood. Different parts of objects, their relative positions within scenes and the relationship of textural patterns extracted from different objects in the same scene are some of the high-level information which can facilitate easier and more accurate detection and recognition of patterns or objects, leading ultimately to a more reliable diagnosis. However, efficient methods of creating or extracting high-level context information, together with image texture features, are currently not available, and this may prove to be a difficult problem [27]. Hence, the notion of using high-level information to solve the CAD problem is still somewhat premature. To our knowledge, the only global feature that is commonly extracted and used in CAD systems is the location or "geography" of a pattern. This is usually done by encoding the positions of patterns or region of interests, by linking them with corresponding anatomical locations or regions. For instance, the feature extraction step can link an abnormality to the right upper or left lower lobe of the lung, or identify it as central or peripheral, helping to further differentiate types of diseases [28, 29]. Figure 1 shows an example for the anatomical compartments and segments of the lungs. Incorporating knowledge of these anatomical regions into clinical practice could help to improve the differentiation of diseases and the quantification of disease progression.

5.1.3. Clinical parameters—Radiologists can be aided in the decision-making process by knowledge of a patients age and gender, the duration and severity of symptoms, the patients body temperature and immune status, and a history of underlying malignancy, smoking, drug treatment, or dust exposure [7, 9, 16]. This information can also be incorporated into a CAD system, but a careful correlation study between clinical and imaging findings will be necessary.

Figure 2 gives an overview of various feature sets that can be used to model CAD systems for lung diseases. None has yet been developed for CAD of respiratory tract infections. However, because of the close similarity between the visual appearances of infectious and inflammatory diseases, we conclude that feature sets and classification methods used to assess inflammatory conditions can also be applied to pulmonary infections. An intriguing question at this point is whether the observed or extracted patterns can be used to discriminate specific diseases. Because textural information alone may not be able to uniquely identify a disease, answering this question may require a correlation of the imaging features with the patients history and clinical findings. This situation is reflected in the low rate of inter-operator agreement in classifying lung diseases [30]. Nevertheless, textures are still important attributes for characterizing and distinguishing objects, lesions, and regions in lung parenchyma, and they could be used effectively to help radiologists, in the way that CAD has been employed in several studies of lung nodules [3, 6, 12, 31–35].

5.2. Radiography and CT patterns and their detection

This section briefly summarizes the most common textural patterns of respiratory tract infections in CT images and chest radiographs. For each finding, we present the use of feature extraction as part of the CAD system, and discuss current state-of-the art feature extraction methods, with their advantages and disadvantages.

5.2.1. Reticular or linear abnormalities—Reticular patterns are small linear opacities, usually perceived as a net, that are seen both in chest radiographs and in CT scans [36]. High resolution CT scans can discriminate different types of reticular patterns, such as interlobular septal thickening, intralobular lines, or cyst walls of honeycombing [36] (See Figure 4.a). If micronodules are superimposed onto reticular opacities, the resulting pattern is called reticulonodular. Reticular opacities are usually seen in interstitial lung diseases; however, their existence in CT and radiograph scans can indicate the presence of an

infectious process, such as in upper or lower respiratory viral infections of adults [37]. For example, influenza C virus can produce a pneumonia that is manifested in radiographs as diffuse, bilateral reticulonodular areas of increased opacity [37]. If the disease progresses, follow-up scans will most probably show diffuse bilateral consolidation. CT scans from a person infected from influenza virus (type C) show GGOs with some irregular linear areas (reticular patterns) of increased attenuation in both lungs.

Computerized detection of reticular opacities: Shape-based features such as thickness, size, area and volume can be effectively used to identify linear and reticular opacities in the lung, such as the thickness of bronchial walls and the sizes of pulmonary arteries adjacent to the bronchi. The reason for using these features is straightforward: reticular patterns consist of lines or straight or elongated ribbon-like formations, caused by thickening of the interstitial fiber network [38]. In addition to shape-based feature extraction methods, the idea of representing textures by their responses to a bank of filters has been developed to detect complex structures that are not easily identified by either method alone [39]. For example, it has been demonstrated that textures can be classified using the joint distribution of intensity values over extremely compact neighbourhoods, outperforming classification using filter banks with large support [40]. More recently, wavelet features and those based on spatial/frequency analysis (Gabor, Local Binary Patterns, Spherical Harmonics, etc.) have received great interest in extracting local texture and shape information, because of their power in analyzing spectral and spatial information. Likewise, the tight fusion between the human visual system and multi-scale filter banks is well known to texture analysis, and efforts have been made to apply it to several CAD systems [14, 28, 29, 41–46]. Spatial/frequency analysis-based features in general offer a variety of scale and frequency bands from which many features can be extracted and the most useful selected. Researchers are now trying to determine how to exploit these features to maximize benefits in terms of texture classification performance [47].

5.2.2. Nodular abnormalities—Nodules and nodular patterns are seen both in chest radiographs and in CT scans. A single nodule has the appearance of a rounded or irregular opacity, which may be well or poorly defined; solid, non-solid or partly solid; and of soft tissue or GGO; usually with a diameter less than 3 cm [36]. Likewise, nodular patterns have numerous small, rounded, discreet opacities, ranging from 2–10 mm in diameter, spread over the lung regions. In contrast, micro-nodules are less than 3 mm in diameter. Non-solid or partly solid nodules may also be seen in combination with GGO; this finding is most likely to be due to an infection in the lung. While a solid nodule has homogeneous soft-tissue attenuation, partly solid nodules include both GGO and solid soft-tissue attenuation. These features can be used to characterize them as being benign or malignant, such that solid nodules are less likely to be malignant compared to partly-solid nodules. Another important factor for making an accurate diagnosis is the distribution of nodules in CT images or chest radiographs. For instance, a centrilobular distribution may indicate infectious airways diseases such as endobronchial spread of tuberculosis (TB), while a random distribution suggests hematogenous metastases, miliary TB, or miliary fungal infections. Figures 3.b and c illustrate examples of nodular patterns seen in chest CT scans.

Computerized detection of nodules and nodular patterns: Shape-based features are often used to detect nodular patterns in chest radiographs and CT scans. Published reports indicate that size, volume, area, diameter, circularity for 2D, form factor, solidarity [48, 49], thickness, top-hat filtering, mean curvature [38], shape index, Gaussian curvature, sphericity for 3D [50–52], surface smoothness, shape irregularity [53], roundness, center of mass [54], compactness, inertia matrix [55], and surface curvature [56] are the most effective and useful features for characterizing nodular patterns. For example, lung nodules come in two

basic shapes: solid and GGO (partly solid and nonsolid). In order to discriminate GGO nodules, which are much more likely to be malignant [57], from solid nodules, a shape feature can be used to define sphericity, solidity or circularity/roundness criteria [50] based on the fact that GGO nodules have more irregular shapes and less well defined boundaries than solid nodules. Fractal-based features can also be used to define geometric similarities between normal and abnormal patterns [58]. For example, benign and malignant tumors in chest radiographs were differentiated using fractal features [59]. The geometric self-similarity of pulmonary blood vessels and the branching structure of the airways facilitate the use of fractal dimension in discriminating normal lung from linear disease features in chest CT scans [60]. However, because chest radiographs and CT scans invariably contain other normal linear and branching structures that are superimposed on one another, presenting a pattern of irregular shapes, the success of fractal-based features is limited.

5.2.3. Altered attenuation (Consolidation)—Consolidation appears in CT scans and chest radiographs when alveolar air has been replaced by an exudate or other product of disease [36]. The homogeneous opacification of the pulmonary parenchyma is preceded by an increase in attenuation, such that bronchial and vascular margins are obscured [61]. Consolidation is not a disease-specific pattern, and it may be seen in different kinds of lung diseases. It has recently been reported that consolidation is almost a common textural pattern in CT scans of patients with novel swine-origin H1N1 influenza [61–66]. Consolidation is also a common pattern found in chest radiographs of patients with Q fever pneumonia [67]. Pulmonary TB is also identified through consolidation and cavities in chest radiographs and tree-in-bud patterns in CT scans [68]. Non-tuberculous mycobacterial infections can also produce consolidation patterns in CT scans. Figure 3.a shows example of dense consolidation in patients with H1N1 influenza.

Computerized detection of consolidation: A co-occurrence matrix has been shown to be very effective for characterizing random textures, and ultimately in use for various CAD systems [38, 48, 49, 56, 69–71], particularly for the detection of consolidation and GGO. Co-occurrence matrices, known also as second-order statistical features, represent the statistical nature of texture for given image blocks by creating a spatial-dependent probability distribution matrix. A standard work has recommended 14 textural features: angular second moment, contrast, correlation, variance, inverse difference moment, sum average, sum variance, entropy, sum entropy, difference variance, difference entropy, two features of information measures of correlations, and maximal correlation coefficient [19]. Meanwhile, run-length features can be defined under the same class with co-occurrence matrix based features, even though it has been shown that they are the least efficient features among a group of traditional texture features [72].

5.2.4. Altered attenuation (Ground-glass opacities (GGO))—The GGO pattern is a common finding on CT scans and chest radiographs, and it is not specific for particular lung diseases. On CT scans and chest radiographs, a GGO is an area of hazy increased density that does not obscure bronchial and vascular margins. The main causes of GGO are partial filling of airspaces, increased capillary blood volume, thickening, collapse of alveoli, or a combination of these [36, 73]. Together with certain clinical tests, the presence of GGO can indicate a specific diagnosis. For example, together with an appropriate clinical history, the combination of GGO and reticular opacities indicates a diagnosis of nonspecific interstitial pneumonia (NSIP) [73, 74]. Similarly, GGO and traction bronchiectasis usually represents fibrosis. GGO are also seen in many different inflammatory and infectious processes. for example, chest radiographs and CT scans of patients with fatal H1N1 influenza contain bilateral areas of mixed GGO and airspace consolidation, predominantly in peripheral and subpleural distributions (Figure 4.b) [63, 65, 66].

Computerized detection of GGO: Areas of GGO can be detected based on a variety of textural features, including image histogram, first-order features, mean and variance of intensities, and kurtosis. Because these basic textural features describe the frequency of occurrence of all the grey levels in a region of interest, they may provide quantitative measures of the degree of pulmonary diseases as stated in [75, 76], in particular for GGO detection, as indicated in [77]. Mean and variance information for grey-level images helps radiologists to track how grey-level information varies among diseases, while kurtosis measures the frequency of the observed patterns and entropy measures the information content of the image [71].

Although it is a challenging problem to find an optimal method of detecting GGO or GGO nodules using only first-order statistical features, some studies have shown promising results if used with carefully designed multi-thresholding methods [77]. As another example, biologically motivated Gabor [78] and Laplacian of Gaussian (LoG) filters have been used to describe the image textures of radiography scans in multi-scale representations [14], suggesting that complex patterns such as GGOs can be extracted in efficient ways by taking into account their size and distribution in the scene. In particular, Gabor filters have been shown to be optimal for minimizing joint two-dimensional uncertainty in space and frequency [78]. However, most existing studies of the selection of the most useful features, such as Gabor features, are empirical rather than optimal.

5.2.5. Altered attenuation (Cavities)—Cavities are gas-filled spaces that sometimes contain fluid. They are usually formed by the expulsion or drainage of a necrotic portion of a lesion through the bronchial tree [36]. Cavities may appear within areas of consolidation, masses or nodules. In many infectious diseases, chest radiographs and CT scans show cavities with consolidation and tree-in-bud patterns, respectively [68]. Lung cavities are most often caused by an infection, such as a fungal disease or tuberculosis. However, cystic fibrosis, sarcoidosis and cancer can also produce cavities.

Computerized detection of cavities: Histogram-based approaches and variations of gradient information are often used to detect cavities in chest radiographs. For more sophisticated cavity-detection problems in CT images, shape-based and texture-based methods can be combined and used as a hybrid approach, similar to the way it has been utilized for chest radiographs [79].

5.2.6. Mixtures (Tree-in-Bud)—As its name implies, this pattern resembles a budding tree in CT scans (See Figure 4.c). It is usually pronounced in centrilobular branching structures in the lung periphery, associated with diseases of the small airways [36]. The tree-in-bud sign indicates bronchiolar luminal impaction with mucus, pus, or fluid, causing normally invisible peripheral airways to become visible [80]. It is not specific for a single disease entity, but is a direct sign of various diseases of the peripheral airways and an indirect sign of bronchiolar diseases, such as air trapping or sub-segmental consolidation. Because any organism that infects the small airways can cause a tree-in-bud pattern, pulmonary infections are its most common cause [80, 81]. This observation is supported by recent studies of thoracic CT findings in patients with novel H1N1 influenza [63, 82, 83]. Patients with pulmonary TB also frequently show tree-in-bud and nodular textural patterns (i.e. micro-nodules) in HRCT scans [84].

Computerized detection of tree-in-bud pattern: There are many technical obstacles to detecting complex shape patterns such as tree-in-bud that are associated with pulmonary infections. Not only are these patterns difficult to detect, but micro-nodules and other normal and abnormal structures have strong shape and appearance similarities with existing structures in the lungs, or they appear as a mixture of normal and abnormal patterns.

Because it has not been easy to learn complicated shapes and configurations using only shape-, texture-, and location-based features are combined seamlessly in implicit ways for many CAD systems that detect complex structures other than tree-in-bud patterns. Because no current CAD system is capable of automatically detecting a tree-in-bud pattern, there is a need to develop such a system to improve the diagnosis of respiratory tract infections.

6. Computerized classification of disease

Ideally, a comprehensive CAD algorithm extracts texture and/or shape features from images and trains them with classifiers to learn discriminative properties of the features (Figure 5). This learnt information is used later in the detection step to classify a texture/shape feature for any given test image. The most commonly used classifiers in CAD systems are nearest-neighbour matching (k-NN), neural networks (NN) or artificial neural network (ANN), Bayesian modelling, rule-based schemes, decision trees, linear discriminant analysis (LDA) and support vector machines (SVM) [14, 29, 46, 49, 70, 71, 85–87]. Among these classifiers, the superiority of SVMs for texture classification has been clearly demonstrated [88, 89]. However, because of their simple implementation, rule-based, Bayesian and nearest-neighbour classification methods are still in use. Furthermore, for complex classifiers such as SVM and ANN, it is necessary to tune numerous parameters to obtain the best phase of the classifiers. Apart from the computational cost, other criteria that affect the choice of classifiers include the complexity of the overall system and the size and type of the data set, so that a theoretically optimal classifier may not be the best practical choice. The strengths and weaknesses of these classifiers are summarized in Table 2. Figure 6 illustrates the organizational principles of the most commonly used classifiers for CAD systems.

6.1. Evaluation of CAD systems

The evaluation of a complete CAD system includes two different performance measures. The first tests the correctness of a computer algorithm, by using data from the training step to produce an output entirely from appropriate detection/classification schemes. In the second level, the final decision about detection/diagnosis is made by expert radiologists who use the computer output as an aid or “second opinion” in their interpretations. The overall performance level of a CAD system is therefore equal to the performance achieved by the radiologist who uses the system in making his final decision [3, 16].

Diagnostic accuracy is tested via the traditional measures of sensitivity and specificity [90, 91], which form the basis for the commonly used receiver operating characteristics (ROC) method of evaluation. In ROC analysis, the observer classifies each image as normal or abnormal, and he may also rate the extent of the abnormality. Because there are two discrete cases (disease or non-disease), there are four possible outcomes. The sensitivity, also called the true-positive fraction (TPF), describes the fraction of diseased patients who are correctly classified by radiologists, while the specificity, also known as the true-negative fraction (TNF), describes the fraction of non-diseased patients who are correctly classified [91]. The other two parameters are the false-positive fraction (FPF), which denotes the fraction of non-diseased patients who are incorrectly classified as diseased, and the false-negative fraction (FNF), the fraction of diseased patients who are incorrectly classified by radiologists as non-diseases. Based on these criteria, a highly accurate CAD system will have high sensitivity and specificity, as independent variables. In ROC analysis, a curve is plotted with TPF (sensitivity) on the y-axis and FPF (1-specificity) on the x-axis. A ROC curve thus indicates the relative trade-offs between benefits (true positives) and costs (false positives) [92].

Overall Accuracy is another term traditionally used to describe the usefulness of a CAD system. It is defined as a summation of true positives and true negatives, normalized over all

diseased and non-diseased patients. Overall accuracy and A_z both fit well to clinical applications involving binary decision tasks. However, if the clinical task does not fit the binary model, precise evaluation through ROC analysis is compromised [98]. The complete analysis of the advantages and limitations of ROC-based methods is beyond the scope of this paper. For further reading on ROC analysis in the setting of CAD, see [86, 90–108].

In Tables 3,4, and 5, we summarize a number of published studies of pulmonary diseases (mainly non-infectious) that display textural and shape patterns similar to those seen in respiratory tract infections. For each study, the tables note the imaging modality, the features extracted from the scans, the classifiers used in the CAD systems and the reported performance, with evaluation criteria. Most of the studies are based on ROC analysis, and report their success rate on the basis of sensitivity, specificity, and A_z. Overall accuracy is another criterion used for evaluation purposes.

6.2. Quantification

Because the textural patterns that identify infectious diseases are diffuse, rather than focal, their quantification is challenging even for an expert radiologist. Although there is no generally accepted, state-of-the-art method for quantifying the extent of lung disease in CT and radiograph scans, a few commonly used methods such as subjective visual examination, semi-automated quantification using morphological filtering and thresholding of grey level histograms are reported in the literature. All of these methods are based on subjective visual evaluation, but quantification of complex image features requires more sophisticated methods. Features pertaining to respiratory tract infections, such as consolidation, GGO and reticular patterns are non-specific; hence, in the following subsections we describe the methods used to stage and determine the rate of progression for a variety of lung diseases.

6.2.1. Visual examination—The most widely used technique of quantifying the extent of pulmonary disease is visual examination, expressed either using a score-based system or as the percentage of lung involvement [1]. Visual examination is simple and fast, but inter-observer variation is high. Although there have been attempts to develop more objective methods, they are currently limited to a few diseases, such as the quantification of emphysema with density mask and correlation with pulmonary functional tests [109]. The co-existence of other lung diseases with mixed patterns, artefacts, and fuzzy areas with non-specific textures (normal or abnormal) can considerably degrade the reliability of objective quantification. Apart from density changes, CT density histograms can also be used to quantify certain conditions (e.g. interstitial lung diseases), for which the density histogram is more peaked and skewed to the left, compared to normal lung. The amount of difference and skewness in density histograms might be used to quantify lung diseases when additional clinical information (e.g. functional tests) is correlated with this finding.

6.2.2. Morphological tools—Subjective visual scoring in pulmonary imaging is strongly operator dependent. Because of significant inter-observer variation, it is highly desirable to quantitatively assess the clinical course [110–112]. The need for quantitative assessment of inflammatory or infectious diseases has led researchers to develop semi-automated methods that combine expert knowledge acquired through visual scoring in training and automatic detection of size, texture and shape patterns using morphological tools. Basically, in the training step, an expert radiologist scores the lung with observed textures such as GGO, and the proportion of each abnormal tissue component and the overall proportion of diseased lung within a pre-defined grid are then obtained by expressing the total score for each component as a percentage of the total number of points scored on each slice or volume.

These methods are only feasible for quantifying certain lung diseases, such as pulmonary fibrosis, under certain conditions, which depend strongly on the scale of the grid. For instance, computing the extent of disease with morphological tools such as a grid may not always give accurate results, because the choice of scale used in the morphometric process is not straightforward. If an inappropriate grid size is chosen, different textural patterns may show similar characteristics. Also, one cannot always use size, volume, or area as quantitative measures for all of the abnormal patterns observed in a scan. For example, large areas of GGO produce large quantitative values in this method, while a small area of consolidation or honeycombing produces a smaller quantitative value. However, it should be noted that GGO is usually considered a reversible process, while consolidation or honeycombing may be irreversible. A visual scoring system that has been optimized through knowledge of disease stage and normal anatomy should therefore be incorporated into the quantification process, in order to compensate for the deficiencies of semi-automated methods.

6.2.3. Quantification through user-defined thresholding—Grey-level thresholding is a simple and efficient method that can be used to extract certain regions from lung parenchyma. The extracted regions and patterns are then filtered by morphological tools to detect the volume, size, and dimensions of pathological regions. Thresholding is often used to identify areas of high attenuation, including GGO and consolidations, and to detect reticular patterns. However, an accurate segmentation of lung parenchyma and airway trees is needed prior to thresholding. Such segmentation can be quite challenging, especially when the lungs contain pathologic abnormalities. Furthermore, the selection of threshold intervals is based entirely on the regional and global distribution of pixel attenuation, as defined by expert users in the training step. Thresholding also is not able to properly separate regions containing both GGO and reticular patterns, resulting in mischaracterization of the nature and extent of disease.

6.3. Other imaging methods

6.3.1. Positron emission tomography—Among the various molecular imaging techniques that could supplement chest radiographs and CT scans for the characterization of respiratory tract infections, PET appears to be the strongest candidate. PET imaging has been used increasingly over the past 30 years to diagnose, stage and monitor malignancies [113]. In pulmonary imaging, for example, it is often necessary to evaluate a nodule or a non-specific opacity for malignancy. Characterization of such focal lung abnormalities with chest radiographs, CT and MRI is a challenging task. In contrast to invasive techniques such as bronchoscopy and biopsy that can assist in diagnosing these abnormalities, PET offers a non-invasive and less expensive means of evaluating lung abnormalities. It has been reported that the use of PET scans in combination with chest radiographs or CT leads to the successful classification of focal pulmonary nodules and other non-specific pulmonary opacities as benign or malignant with a specificity of 80–95% and a sensitivity of 89–100% [114, 115].

Although its use in evaluating pulmonary infections is not well established, Figure 7 shows that PET imaging can detect tree-in-bud patterns. Because such patterns are a strong indicator of infection, PET and CT could potentially be used together to differentiate non-specific patterns observed in CT images. Nevertheless, little use has been made of PET imaging to identify respiratory tract infections, mainly because its efficacy in evaluating pulmonary abnormalities other than focal nodules is still not known. False negatives may also occur due to the relatively limited resolution of PET scans. The optimal algorithm incorporating PET imaging to detect and characterize pulmonary abnormalities has not yet

been identified, but the evolving applications of PET and texture analysis for thoracic imaging appear promising [113, 116].

6.3.2. Ultrasound—Because US can identify vascular structures in real time without using ionizing radiation or requiring the introduction of contrast material, it has attracted the attention of radiologists for many years. US is increasingly used alongside radiography and CT to image lesions of the lung, mediastinum and pleura through anatomical acoustic windows. For example, pleural effusions, a common finding in infectious diseases, can easily be detected by US [117]. Consolidation may also be amenable to US imaging, because the filling of normal air spaces results in the conversion of portions of the lung into solid structures that readily transmit sound. US scanning of infants is facilitated by low bone density. Despite these advantages, US is not routinely used to detect pulmonary infections, due to its inability to correctly classify textural patterns, determine the extent of a deep lesion, visualize an entire region of interest in the chest or identify abnormalities that are neither solid nor fluid [117, 118].

6.3.3. Magnetic resonance imaging—Although MRI allows the acquisition of high-definition images with great sensitivity, it is only rarely chosen as an imaging modality for pulmonary diseases because of its poor specificity. The only setting in which MRI has an advantage over CT is in identifying infections of the pleura and chest wall, for which the use of MRI can minimize radiation exposure and define chest wall involvement [117]. MRI can also be used to characterize fetal chest anatomy during pregnancy, providing more accurate information than US alone and avoiding radiation exposure. In this specific scenario, T2-weighted sequences are the most useful, because the significant volume of fluid in the fetal chest causes the lung signal to be homogeneously high [118]. Although MRI can identify a hydrothorax (abnormal accumulation of fluid in the pleural space), it cannot determine if the condition is caused by infection or by a chromosomal abnormality [118]. Because of its relatively high cost, the frequent need for sedation and poor visualization of the lung parenchyma, the use of MRI is limited. HRCT therefore remains the “gold standard” for imaging pulmonary diseases.

7. Conclusion

CAD systems can be applied to the imaging of respiratory tract infections by following by two basic analyses: imaging findings from infectious diseases in general (i.e. texture and shape patterns) and computerized recognition of those findings in a computational platform. In discussing the first step, we have focused on texture and shape patterns seen in pulmonary infections such as TB or H1N1 influenza. For the second, we have manifested computational tools such as feature extraction and classifier design that are required to design a robust and successful CAD system.

Acknowledgments

This research is supported in part by the Imaging Sciences Training Program (ISTP), the Center for Infectious Disease Imaging (CIDI), and Intramural Research Program of the National Institute of Bio-imaging and Bioengineering at the National Institutes of Health.

References

1. Hansell DM. Imaging the lungs with Computed tomography. IEEE Engineering in Medicine and Biology Magazine. 2000; 19(5):71–79. [PubMed: 11016032]
2. Yao J, et al. Computer-aided diagnosis of pulmonary infections using texture analysis and support vector machine classification. Academic Radiology. 2011; 18(3):306–314. [PubMed: 21295734]

3. Doi K. Computer-aided diagnosis in medical imaging: Historical review, current status and future potential. Computerized Medical Imaging and Graphics. 2007; 31(4–5):198–211. [PubMed: 17349778]
4. Giger ML, et al. Anniversary Paper: History and status of CAD and quantitative image analysis: The role of Medical Physics and AAPM. Medical Physics. 2008; 35(12):5799–5820. [PubMed: 19175137]
5. Summers RM. Road maps for advancement of radiologic computer-aided detection in the 21st century. Radiology. 2003; 229(1):11–13. [PubMed: 14519863]
6. Sluimer I, et al. Computer analysis of computed tomography scans of the lung: A survey. IEEE Transactions on Medical Imaging. 2006; 25(4):385–405. [PubMed: 16608056]
7. van Ginneken B, et al. Computer-aided diagnosis in chest radiography: Beyond nodules. European Journal of Radiology. 2009; 72(2):226–230. [PubMed: 19604661]
8. Way T, et al. Computer-Aided Diagnosis of Lung Nodules on CT Scans: ROC Study of Its Effect on Radiologists' Performance. Academic Radiology. 2010; 17(3):323–332. [PubMed: 20152726]
9. van Ginneken B, et al. Computer-aided diagnosis in chest radiography: A survey. IEEE Transactions on Medical Imaging. 2001; 20(12):1228–1241. [PubMed: 11811823]
10. Joarder, R., et al. Chest X-Ray in Clinical Practice. Springer Verlag London Limited; 2009.
11. Sluimer IC, et al. Automated classification of hyperlucency, fibrosis, ground glass, solid, and focal lesions in high-resolution CT of the lung. Medical Physics. 2006; 33(7):2610–2620. [PubMed: 16898465]
12. Sluimer IC, et al. Computer-aided diagnosis in high resolution CT of the lungs. Medical Physics. 2003; 30(12):3081–3090. [PubMed: 14713074]
13. Abe H, et al. Computer-aided diagnosis in chest radiography: Results of large-scale observer tests at the 1996–2001 RSNA scientific assemblies. Radiographics. 2003; 23(1):255–265. [PubMed: 12533660]
14. Coppini G, et al. Neural networks for computer-aided diagnosis: Detection of lung nodules in chest radiograms. IEEE Transactions on Information Technology in Biomedicine. 2003; 7(4):344–357. [PubMed: 15000360]
15. Doi K, et al. Computer-aided diagnosis in digital chest radiography. Advances in Digital Radiography: RSNA Categorical Course in Diagnostic Radiology Physics 2003 Syllabus 2003. : 227–236.
16. Katsuragawa S, Doi K. Computer-aided diagnosis in chest radiography. Computerized Medical Imaging and Graphics. 2007; 31(4–5):212–223. [PubMed: 17403598]
17. Crosier M, Griffin LD. Using Basic Image Features for Texture Classification. International Journal of Computer Vision. 2010; 88(3):447–460.
18. Kim KI, et al. Support vector machines for texture classification. IEEE Transactions on Pattern Analysis and Machine Intelligence. 2002; 24(11):1542–1550.
19. Haralick RM, et al. Textural Features for Image Classification. IEEE Transactions on Systems Man and Cybernetics. 1973; Smc3(6):610–621.
20. Bovik AC, et al. Multichannel Texture Analysis Using Localized Spatial Filters. IEEE Transactions on Pattern Analysis and Machine Intelligence. 1990; 121:55–73.
21. Teuner A, et al. Unsupervised Texture Segmentation of Images Using Tuned Matched Gabor Filters. IEEE Transactions on Image Processing. 1995; 4(6):863–870. [PubMed: 18290038]
22. Chang T, Kuo CCJ. Texture analysis and classification with tree-structured wavelet transform. IEEE Transactions on Image Processing. 1993; 2(4):429–441. [PubMed: 18296228]
23. Laine A, Fan J. Texture Classification by Wavelet Packet Signatures. IEEE Transactions on Pattern Analysis and Machine Intelligence. 1993; 15(11):1186–1191.
24. Unser M. Texture Classification and Segmentation Using Wavelet Frames. IEEE Transactions on Image Processing. 1995; 4(11):1549–1560. [PubMed: 18291987]
25. Schlachter M, et al. Harmonic Filters for 3D Multichannel Data: Rotation Invariant Detection of Mitoses in Colorectal Cancer. Transactions on Medical Imaging. 2010; 29(8):11.

26. Pun CM, Lee MC. Log-polar wavelet energy signatures for rotation and scale invariant texture classification. IEEE Transactions on Pattern Analysis and Machine Intelligence. 2003; 25(5):590–603.
27. Tu ZW, Bai XA. Auto-Context and Its Application to High-Level Vision Tasks and 3D Brain Image Segmentation. IEEE Transactions on Pattern Analysis and Machine Intelligence. 2010; 32(10):1744–1757. [PubMed: 20724753]
28. Katsuragawa S, et al. Image Feature Analysis and Computer-Aided Diagnosis in Digital Radiography - Detection and Characterization of Interstitial Lung-Disease in Digital Chest Radiographs. Medical Physics. 1988; 15(3):311–319. [PubMed: 3405134]
29. Katsuragawa S, et al. Image Feature Analysis and Computer-Aided Diagnosis in Digital Radiography - Classification of Normal and Abnormal Lungs with Interstitial Disease in Chest Images. Medical Physics. 1989; 16(1):38–44. [PubMed: 2646516]
30. Doi K, Huang HK. Computer-aided diagnosis (CAD) and image-guided decision support. Computerized Medical Imaging and Graphics. 2007; 31(4–5):195–197.
31. Gurcan MN, et al. Lung nodule detection on thoracic computed tomography images: Preliminary evaluation of a computer-aided diagnosis system. Medical Physics. 2002; 29(11):2552–2558. [PubMed: 12462722]
32. Doi K. Current status and future potential of computer-aided diagnosis in medical imaging. British Journal of Radiology. 2005; 78:S3–S19. [PubMed: 15917443]
33. Fukushima A, et al. Application of an artificial neural network to high-resolution CT: Usefulness in differential diagnosis of diffuse lung disease. American Journal of Roentgenology. 2004; 183(2):297–305. [PubMed: 15269016]
34. MacMahon H, et al. Computer-aided diagnosis of pulmonary nodules: Results of a large-scale observer test. Radiology. 1999; 213(3):723–726. [PubMed: 10580945]
35. Shiraishi, et al. Computer-aided diagnosis for improved detection of lung nodules by use of posterior-anterior and lateral chest radiographs. Academic Radiology. 2007; 14(1):28–37. [PubMed: 17178363]
36. Hansell DM, et al. Fleischner Society: Glossary of terms tor thoracic imaging. Radiology. 2008; 246(3):697–722. [PubMed: 18195376]
37. Kim EA, et al. Viral pneumonias in adults: Radiologic and pathologic findings. Radiographics. 2002; 22:S137–S149. [PubMed: 12376607]
38. Shyu CR, et al. ASSERT: A physician-in-the-loop content-based retrieval system for HRCT image databases. Computer Vision and Image Understanding. 1999; 75(1–2):111–132.
39. Mellor M, et al. Locally rotation, contrast, and scale invariant descriptors for texture analysis. IEEE Transactions on Pattern Analysis and Machine Intelligence. 2008; 30(1):52–61. [PubMed: 18000324]
40. Varma M, Zisserman A. Texture Classification: Are Filter Banks Necessary? IEEE International Conference on Computer Vision and Pattern Recognition. 2003:691–698.
41. Ishida T, et al. Computerized analysis of interstitial disease in chest radiographs: Improvement of geometricpattern feature analysis. Medical Physics. 1997; 24(6):915–924. [PubMed: 9198027]
42. Katsuragawa S, et al. Quantitative Computer-Aided Analysis of Lung Texture in Chest Radiographs. Radiographics. 1990; 10(2):257–269. [PubMed: 2326513]
43. Katsuragawa S, et al. Image Feature Analysis and Computer-Aided Diagnosis in Digital Radiography - Effect of Digital Parameters on the Accuracy of Computerized Analysis of Interstitial Disease in Digital Chest Radiographs. Medical Physics. 1990; 17(1):72–78. [PubMed: 2407936]
44. Monniercholley L, et al. Computerized Analysis of Interstitial Infiltrates on Chest Radiographs - a New Scheme Based on Geometric Pattern Features and Fourier-Analysis. Academic Radiology. 1995; 2(6):455–462. [PubMed: 9419591]
45. Morishita J, et al. Computer-Aided Diagnosis for Interstitial Infiltrates in Chest Radiographs - Optical-density Dependence of Texture Measures. Medical Physics. 1995; 22(9):1515–1522. [PubMed: 8531883]

46. van Ginneken B, et al. Automatic detection of abnormalities in chest radiographs using local texture analysis. IEEE Transactions on Medical Imaging. 2002; 21(2):139–149. [PubMed: 11929101]
47. Bagci, U.; Bai, L. Parallel Adaboost Algorithm For Gabor Wavelet Selection in Face Recognition. IEEE International Conference on Image Processing; IEEE; San Diego, CA. 2008. p. 1640-1643.
48. Uchiyama Y, et al. Quantitative computerized analysis of diffuse lung disease in high-resolution computed tomography. Medical Physics. 2003; 30(9):2440–2454. [PubMed: 14528966]
49. Chen H, et al. Neural Network Ensemble-Based Computer-Aided Diagnosis for Differentiation of Lung Nodules on CT Images Clinical Evaluation. Academic Radiology. 2010; 17(5):595–602. [PubMed: 20167513]
50. Ye XJ, et al. Shape-Based Computer-Aided Detection of Lung Nodules in Thoracic CT Images. IEEE Transactions on Biomedical Engineering. 2009; 56(7):1810–1820. [PubMed: 19527950]
51. Monga O, et al. Using Partial Derivatives of 3d Images to Extract Typical Surface-Features. Computer Vision and Image Understanding. 1995; 61(2):171–189.
52. Ye, X., et al. Efficient computer-aided detection of ground-glass opacity nodules in thoracic CT images; Conf Proc IEEE Eng Med Biol Soc; 2007. p. 4449-4452.
53. Way TW, et al. Computer-aided diagnosis of pulmonary nodules on CT scans: Improvement of classification performance with nodule surface features. Medical Physics. 2009; 36(7):3086–3098. [PubMed: 19673208]
54. Golosio B, et al. A novel multi-threshold method for nodule detection in lung CT. Medical Physics. 2009; 36(8):3607–3618. [PubMed: 19746795]
55. Boeroezky L, et al. Feature subset selection for improving the performance of false positive reduction in lung nodule CAD. IEEE Transactions on Information Technology in Biomedicine. 2006; 10(3):504–511. [PubMed: 16871718]
56. Kim KG, et al. Computer-aided diagnosis of localized ground-glass opacity in the lung at CT: Initial experience. Radiology. 2005; 237(2):657–661. [PubMed: 16192320]
57. Chong SM, et al. Lung cancer screening with low-dose helical CT in Korea: Experiences at the Samsung Medical Center. Journal of Korean Medical Science. 2005; 20(3):402–408. [PubMed: 15953860]
58. Iannaccone, PM., et al. Fractal geometry in biological systems : an analytical approach. Boca Raton, FL: CRC Press; 1996. p. 360
59. Peiss J, et al. Classification of lung tumors on chest radiographs by fractal texture analysis. Investigative Radiology. 1996; 31(10):625–629. [PubMed: 8889651]
60. Uppaluri R, et al. Computer recognition of regional lung disease patterns. American Journal of Respiratory and Critical Care Medicine. 1999; 160(2):648–654. [PubMed: 10430742]
61. Henzler T, et al. Image Findings of Patients with H1N1 Virus Pneumonia and Acute Respiratory Failure. Academic Radiology. 2010; 17(6):681–685. [PubMed: 20457412]
62. Agarwal PP, et al. Chest Radiographic and CT Findings in Novel Swine-Origin Influenza A (H1N1) Virus (S-OIV) Infection. American Journal of Roentgenology. 2009; 193(6):1488–1493. [PubMed: 19933638]
63. Mollura DJ, et al. Imaging Findings in a Fatal Case of Pandemic Swine-Origin Influenza A (H1N1). American Journal of Roentgenology. 2009; 193(6):1500–1503. [PubMed: 19933640]
64. Lee EY, et al. Swine-Origin Influenza A (H1N1) Viral Infection in Children: Initial Chest Radiographic Findings. Radiology. 2010; 254(3):934–941. [PubMed: 20032128]
65. Aviram G, et al. H1N1 Influenza: Initial Chest Radiographic Findings in Helping Predict Patient Outcome. Radiology. 2010; 255(1):252–259. [PubMed: 20308461]
66. Guo HH, et al. Best Cases from the AFIP Fatal 2009 Influenza A (H1N1) Infection, Complicated by Acute Respiratory Distress Syndrome and Pulmonary Interstitial Emphysema. Radiographics. 2010; 30(2):327–333. [PubMed: 20068001]
67. Gikas A, et al. Q fever pneumonia: Appearance on chest radiographs. Radiology. 1999; 210(2): 339–343. [PubMed: 10207412]
68. Eun Young Kim, et al. Pulmonary Mycobacterial Disease: Diagnostic Performance of Low-Dose Digital Tomosynthesis as Compared with Chest Radiography. Radiology. 2010; 257:9.

69. Chabat F, et al. Obstructive lung diseases: Texture classification for differentiation at CT. Radiology. 2003; 228(3):871–877. [PubMed: 12869685]
70. Tatjana Zrimec, et al. Improving Computer Aided Disease Detection Using Knowledge of Disease Appearance. In: Kuhn, K., editor. MEDINFO. Vol. 2007. 2007. p. 1324-1328.
71. Xu Y, et al. Computer-aided classification of interstitial lung diseases via MDCT: 3D adaptive multiple feature method (3D AMFM). Academic Radiology. 2006; 13(8):969–978. [PubMed: 16843849]
72. Tang XO. Texture information in run-length matrices. IEEE Transactions on Image Processing. 1998; 7(11):1602–1609. [PubMed: 18276225]
73. Collins J. CT signs and patterns of lung disease. Radiologic Clinics of North America. 2001; 39(6): 1115. [PubMed: 11699664]
74. Collins, J., et al. Chest Radiology. Wolters Kluwer, Lippincot Williams & Wilkins; 2008.
75. Sorensen L, et al. Quantitative Analysis of Pulmonary Emphysema Using Local Binary Patterns. IEEE Transactions on Medical Imaging. 2010; 29(2):559–569. [PubMed: 20129855]
76. Nagao M, et al. Quantitative analysis of pulmonary emphysema: Three-dimensional fractal analysis of single-photon emission computed tomography images obtained with a carbon particle radioaerosol. American Journal of Roentgenology. 1998; 171(6):1657–1663. [PubMed: 9843308]
77. Okada T, et al. Computer-aided diagnosis of lung cancer: definition and detection of ground-glass opacity type of nodules by high-resolution computed tomography. Japanese Journal of Radiology. 2009; 27(2):91–99. [PubMed: 19373538]
78. Manjunath BS, et al. Texture features for browsing and retrieval of image data. IEEE Transactions on Pattern Analysis and Machine Intelligence. 1996; 18(8):837–842.
79. Shen R, et al. A Hybrid Knowledge-Guided Detection Technique for Screening of Infectious Pulmonary Tuberculosis From Chest Radiographs. IEEE Transactions on Biomedical Engineering. 2010; 57(11):2646–2656.
80. Eisenhuber E. The tree-in-bud sign. Radiology. 2002; 222(3):771–772. [PubMed: 11867799]
81. Aquino SL, et al. Tree-in-bud pattern: Frequency and significance on thin section CT. Journal of Computer Assisted Tomography. 1996; 20(4):594–599. [PubMed: 8708063]
82. Elicker BM, et al. Thoracic CT Findings of novel influenza A (H1N1) infection in immunocompromised patients. Emergency Radiology. 2010; 17(4):9.
83. Abbo L, et al. Pulmonary imaging of pandemic influenza H1N1 infection: relationship between clinical presentation and disease burden on chest radiography and CT. British Journal of Radiology. 2010; 83(992):645–651. [PubMed: 20551254]
84. Lee ES, et al. Computed Tomography Features of Extensively Drug-Resistant Pulmonary Tuberculosis in Non-HIV-Infected Patients. Journal of Computer Assisted Tomography. 2010; 34(4):559–563. [PubMed: 20657225]
85. Penedo MG, et al. Computer-aided diagnosis: A neural-network-based approach to lung nodule detection. IEEE Transactions on Medical Imaging. 1998; 17(6):872–880. [PubMed: 10048844]
86. Yoon HJ, et al. Evaluating computer-aided detection algorithms. Medical Physics. 2007; 34(6): 2024–2038. [PubMed: 17654906]
87. Arzhaevaa Y, et al. Computer-aided detection of interstitial abnormalities in chest radiographs using a reference standard based on computed tomography. Medical Physics. 2007; 34(12):4798–4809. [PubMed: 18196808]
88. Hayman E, et al. On the significance of real-world conditions for material classification. Computer Vision - ECCV. 2004; (Pt 4):253–266. 2004. 2034.
89. Zhang J, et al. Local features and kernels for classification of texture and object categories: A comprehensive study. International Journal of Computer Vision. 2007; 73(2):213–238.
90. Fawcett T. An introduction to ROC analysis. Pattern Recognition Letters. 2006; 27(8):861–874.
91. van Erkel AR, et al. Receiver operating characteristic (ROC) analysis: Basic principles and applications in radiology. European Journal of Radiology. 1998; 27(2):88–94. [PubMed: 9639133]
92. Wagner RF, et al. Assessment of medical imaging systems and computer aids: A tutorial review. Academic Radiology. 2007; 14(6):723–748. [PubMed: 17502262]

93. Metz CE. Roc Methodology in Radiologic Imaging. Investigative Radiology. 1986; 21(9):720–733. [PubMed: 3095258]
94. Dwyer AJ. In pursuit of a piece of the ROC. Radiology. 1996; 201(3):621–625. [PubMed: 8939207]
95. Dorfman DD. Multireader, multicase receiver operating characteristic methodology: A bootstrap analysis. Academic Radiology. 1997; 4(2):107.
96. Bradley AP. The use of the area under the ROC curve in the evaluation of machine learning algorithms. Pattern Recognition. 1997; 30(7):1145–1159.
97. Hanley JA, et al. The Meaning and Use of the Area under a Receiver Operating Characteristic (ROC) Curve. Radiology. 1982; 143(1):29–36. [PubMed: 7063747]
98. Chakraborty D. Statistical power in observer-performance studies: Comparison of the receiver operating characteristic and free-response methods in tasks involving localization. Academic Radiology. 2002; 9(2):147–156. [PubMed: 11918367]
99. Chakraborty DP, et al. Validation and Statistical Power Comparison of Methods for Analyzing Free-response Observer Performance Studies. Academic Radiology. 2008; 15(12):1554–1566. [PubMed: 19000872]
100. Sahiner B, et al. Joint two-view information for computerized detection of microcalcifications on mammograms. Medical Physics. 2006; 33(7):2574–2585. [PubMed: 16898462]
101. Pesce LL, et al. On the Convexity of ROC Curves Estimated from Radiological Test Results. Academic Radiology. 2010; 17(8):960–968. [PubMed: 20599155]
102. Shiraishi J, et al. Experimental Design and Data Analysis in Receiver Operating Characteristic Studies: Lessons Learned from Reports in Radiology from 1997 to 2006. Radiology. 2009; 253(3):822–830. [PubMed: 19864510]
103. Edwards DC, et al. Optimization of restricted ROC surfaces in three-class classification tasks. IEEE Transactions on Medical Imaging. 2007; 26(10):1345–1356. [PubMed: 17948725]
104. He X, et al. Three-class ROC analysis - A decision theoretic approach under the ideal observer framework. IEEE Transactions on Medical Imaging. 2006; 25(5):571–581. [PubMed: 16689261]
105. Edwards DC, et al. Maximum likelihood fitting of FROC curves under an initial-detection-and-candidate-analysis model. Medical Physics. 2002; 29(12):2861–2870. [PubMed: 12512721]
106. MacEneaney PM, et al. ROC curves for the 21st century: Adding a third dimension to incorporate the anatomic extent of disease. Radiology. 2001; 221:426–426.
107. Lipton MJ, et al. Cost-effectiveness in radiology. European Radiology. 2000; 10:S390–S392. [PubMed: 11001454]
108. Metz CE, et al. Proper binormal ROC curves: Theory and maximum-likelihood estimation. Journal of Mathematical Psychology. 1999; 43(1):1–33. [PubMed: 10069933]
109. Kinsella M, et al. Quantitation of emphysema by computed tomography using a density mask program and correlation with pulmonary function tests. Chest. 1990; 97(2):315–321. [PubMed: 2298057]
110. Rodriguez LH, et al. Automated Discrimination and Quantification of Idiopathic Pulmonary Fibrosis from Normal Lung Parenchyma Using Generalized Fractal Dimensions in High-Resolution Computed-Tomography Images. Academic Radiology. 1995; 2(1):10–18. [PubMed: 9419518]
111. Watters LC, et al. A Clinical, Radiographic and Physiologic Scoring System for the Longitudinal Assessment of Patients with Idiopathic Pulmonary Fibrosis. American Review of Respiratory Disease. 1986; 133:97–103. [PubMed: 3942381]
112. Leung AN, et al. Parenchymal opacification in chronic infiltrative lung disease: CT - pathologic correlation. Radiology. 1993; 186:209–214. [PubMed: 8511299]
113. Lowe VJ, et al. Current role of positron emission tomography in thoracic oncology. Thorax. 1998; 53(8):703–712. [PubMed: 9828860]
114. Dewan NA, et al. Diagnostic Efficacy of PET-FDG Imaging in Solitary Pulmonary Nodules - Potential Role in Evaluation and Management. Chest. 1993; 104(4):997–1002. [PubMed: 8404239]

115. Patz EF, et al. Focal Pulmonary Abnormalities - Evaluation with F-18 Fluorodeoxyglucose Pet Scanning. Radiology. 1993; 188(2):487–490. [PubMed: 8327702]
116. Yu H, et al. Coregistered FDG PET/CT-Based Textural Characterization of Head and Neck Cancer for Radiation Treatment Planning. IEEE Transactions on Medical Imaging. 2009; 28(3): 374–383. [PubMed: 19244009]
117. Davies HE, et al. Management of pleural infection in adults: British Thoracic Society pleural disease guideline 2010. Thorax. 2010; 65:41–53.
118. Baert, AL., et al. Pediatric Chest Imaging: Chest Imaging in Infants and Children. 2nd ed. Lucaya, J.; Strife, JL., editors. Springer; 2007. p. 450
119. http://www.imaios.com e-Anatomy. [cited 2010 06 October].
120. Arzhaeva Y, Prokop M, Murphy K, van Rikxoort EM, de Jong PA, Gietema HA, et al. Automated estimation of progression of interstitial lung disease in CT images. Medical Physics. 2010; 37(1):63–73. [PubMed: 20175467]
121. Asada N, Doi K, MacMahon H, Montner SM, Giger ML, Abe C, et al. Potential usefulness of an artificial neural network for differential diagnosis of interstitial lung diseases: pilot study. Radiology. 1990; 177(3):857–860. [PubMed: 2244001]
122. Abe H, Ashizawa K, Katsuragawa S, MacMahon H, Doi K. Use of an artificial neural network to determine the diagnostic value of specific clinical and radiologic parameters in the diagnosis of interstitial lung disease on chest radiographs. Academic Radiology. 2002; 9(1):13–17. [PubMed: 11918354]
123. Caban JJ, Yao J, Avila NA, Fontana JR, Manganiello VC. Texture Based Computer Aided Diagnosis System for Lung Fibrosis. Proc. Of SPIE Medical Imaging. 2007; 651439:1–4.
124. Kauczor HU, Heitmann K, Heussel CP, Marwerde D, Uthmann T, Thelen M. Automatic detection and quantification of ground-glass opacities on high-resolution CT using multiple neural networks: Comparison with a density mask. American Journal of Roentgenology. 2000; 175(5):1329–1334. [PubMed: 11044035]
125. Korfiatis P, Kalogeropoulou C, Karahaliou A, Kazantzi A, Skiadopilos S, Costaridou L. Texture classification-based segmentation of lung affected by interstitial pneumonia in high-resolution CT. Medical Physics. 2008; 35(12):5290–5302. [PubMed: 19175088]
126. Arzhaeva Y, Prokop M, Murphy K, van Rikxoort EM, de Jong PA, Gietema HA, et al. Automated estimation of progression of interstitial lung disease in CT images. Medical Physics. 2010; 37(1):63–73. [PubMed: 20175467]
127. Kauczor HU, Heitmann K, Heussel CP, Marwede D, Uthmann T, Thelen M. Automatic detection and quantification of ground-glass opacities on high-resolution CT using multiple neural networks: Comparison with a density mask. American Journal of Roentgenology. 2000; 175(5): 1329–1334. [PubMed: 11044035]
128. Cheng HD, Shi XJ, Min R, Hu LM, Cai XP, Du HN. Approaches for automated detection and classification of masses in mammograms. Pattern Recognition. 2006; 39(4):646–668.

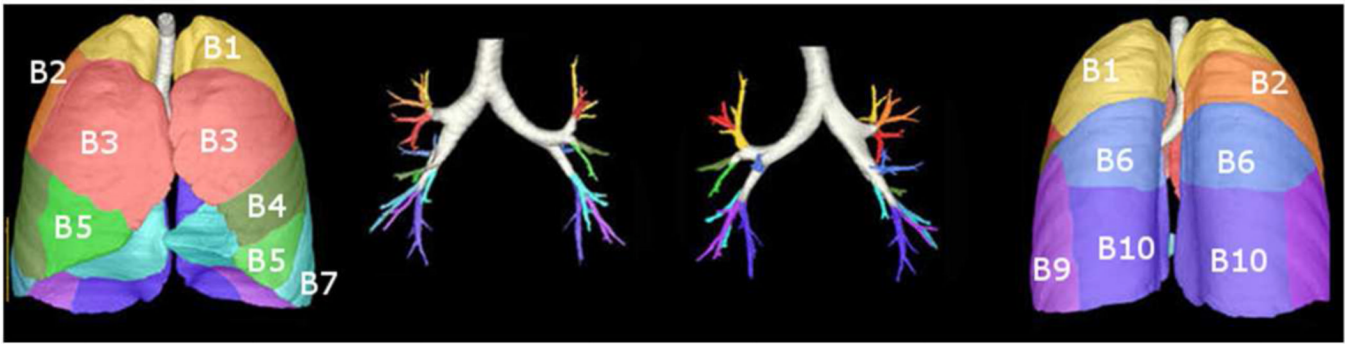

Figure 1.
Anatomical lung segments: B1: Apical, B2: Posterior, B3: Anterior, B4: Lateral, B5: Medial, B6: Superior, B7: Basal Medial, B8: Basal Anterior, B9: Basal Lateral, B10: Basal Posterior (Partly from [119], with permission).

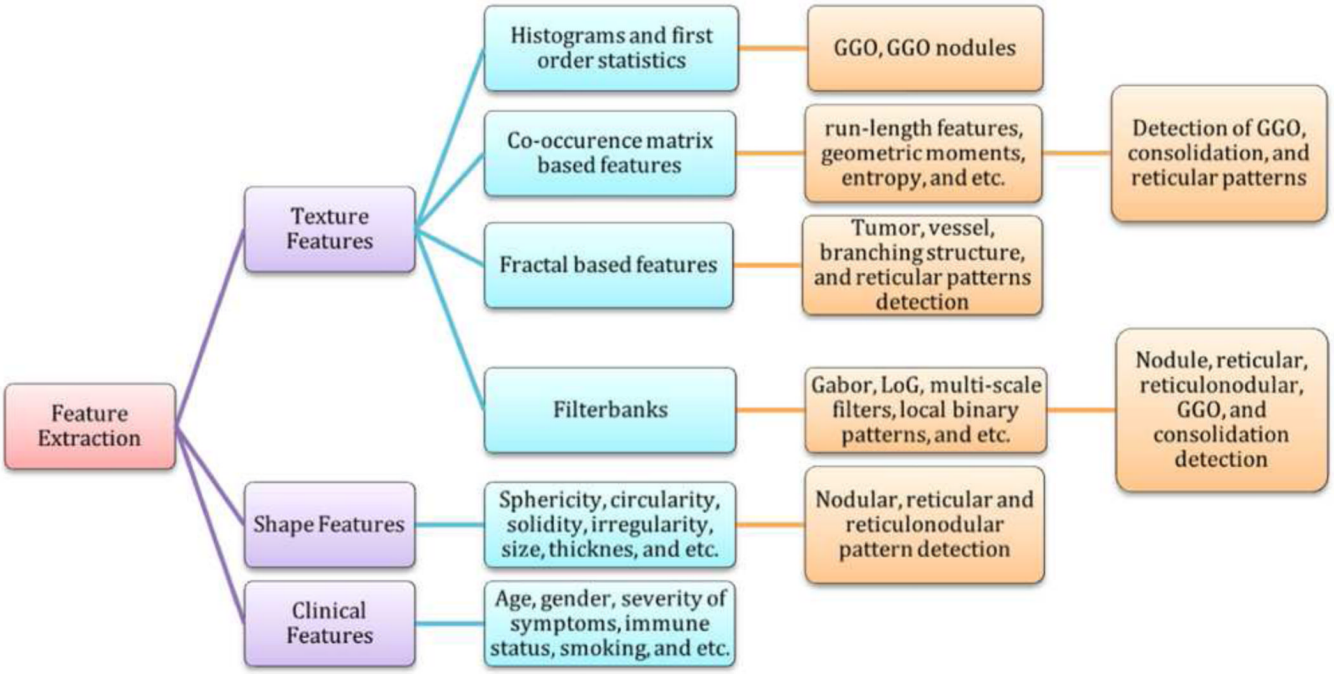

Figure 2.
Overview of different feature sets used in CAD systems for lung diseases.

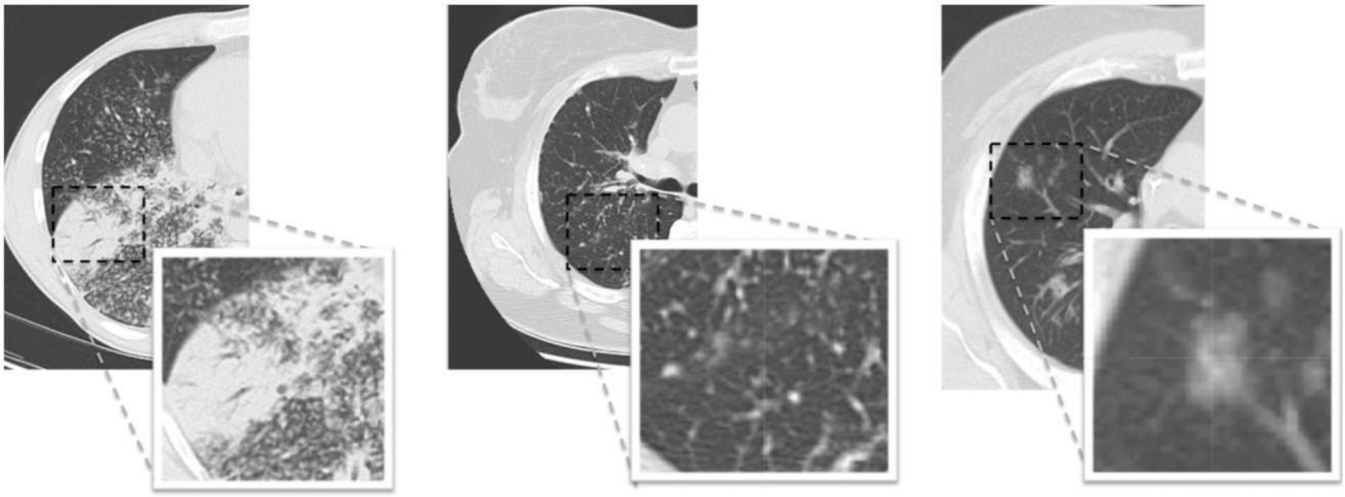

Figure 3.
a. Consolidation, b. nodules and nodular structures, c. ground glass nodular opacities.

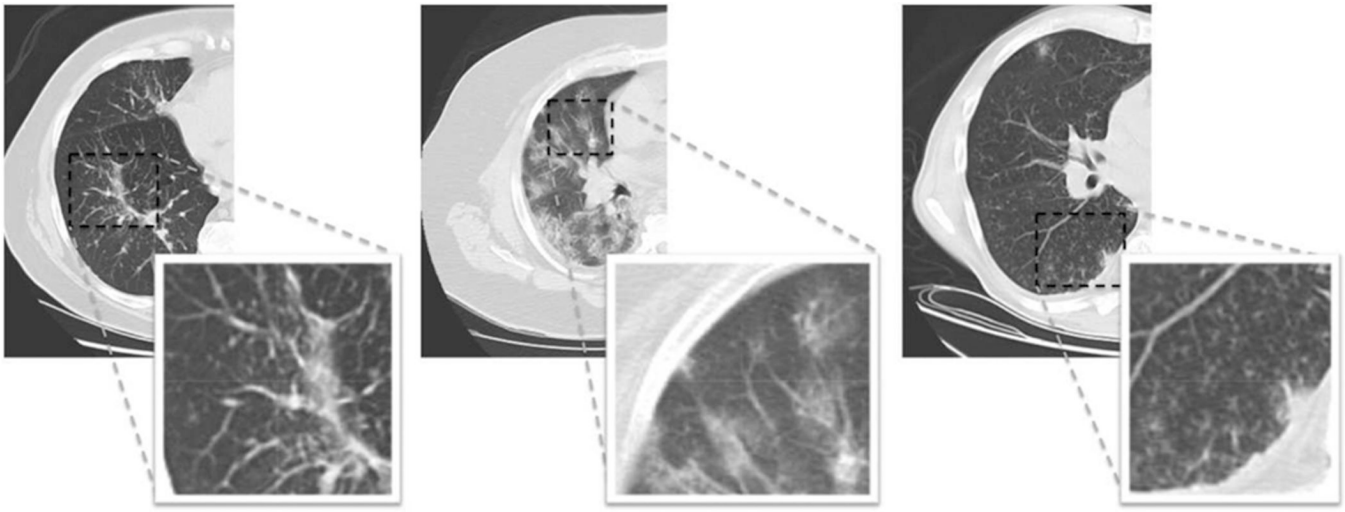

Figure 4.
(a) Reticular, (b) GGO, (c) tree-in-bud patterns.

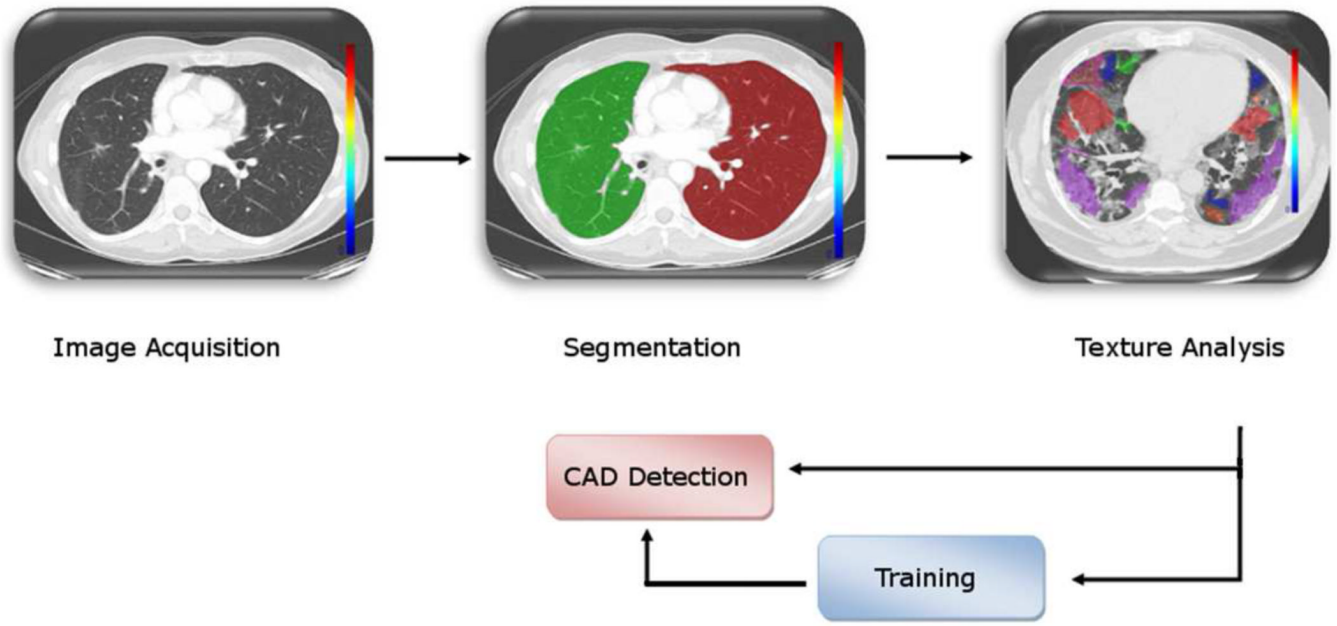

Figure 5.
An example of a CAD system using CT scans. Texture analysis is based on manual labelling of textures or shapes.

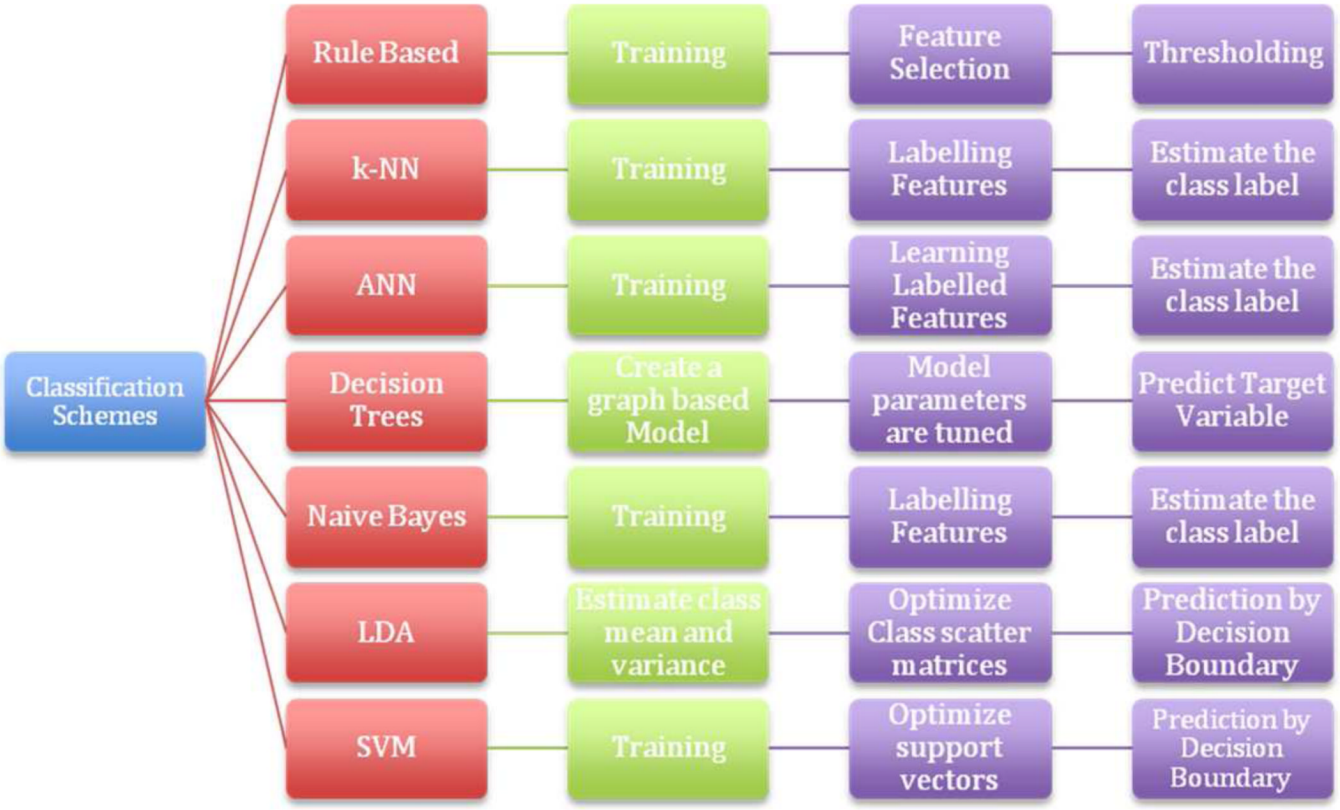

Figure 6.
The most commonly used classifiers for CAD systems, with their organizational principles.

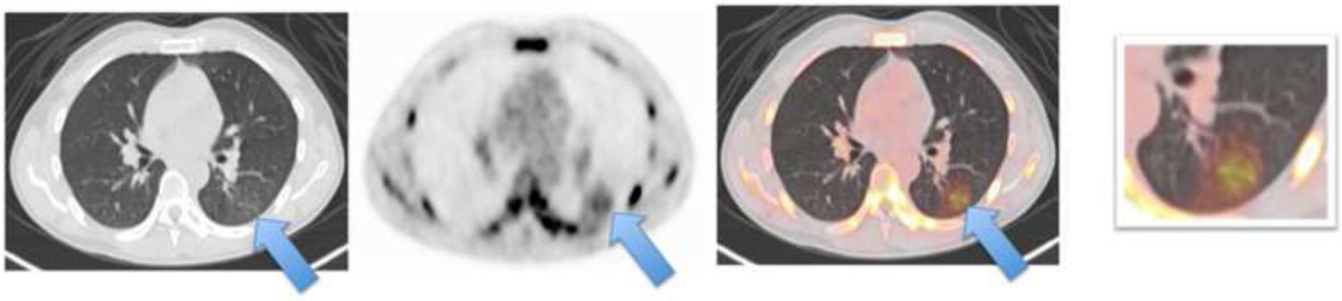

Figure 7.
Tree-in-bud detection with PET imaging (Left: CT, Middle: PET, Right: superimposed PET-CT, Rightmost: zoomed)

Table 1

Characteristic patterns of chest radiography and CT imaging.

General feature	Examples
Reticular or linear abnormality	• Septal thickening (smooth, irregular or nodular) • Bronchovascular thickening
Nodular abnormality	• Miliary Centrilobular Perilymphatic
Altered attenuation	• Increased attenuation (GGO) • Decreased attenuation (cysts, emphysema, cavities, honeycombing) • Mosaic (primary vascular, primary airway, patchy infiltrative lung disease
Mixture	• Tree-in-bud and Crazy paving

Table 2

Advantages and disadvantages of the classifiers most commonly used in CAD systems.

Classifier	Advantages	Disadvantages
Rule-based	Simple to implement, and can be integrated into k-NN, ANN or decision trees.	Selection of cutoff threshold to classify abnormal and normal is manual, hence suboptimal [125].
k-NN	Gives consistent classification results. Consistency increases with the amount of data.	Finding an optimal value for “k” is challenging [44–108]. A large dataset is needed.
ANN	Have ability to learn complex input-output relationships, and have low dependence on domain specific knowledge [126].	Need numerous parameters to tune classifiers. Computational complexity is high, and overtraining is often inevitable.
Decision Trees	Low computational complexity. Can be integrated into other classifiers. Less extensive prior information is necessary [127].	Not guaranteed to have a globally optimal solution. Pruning the data is needed to avoid over-fitting.
Naïve Bayes	Optimal with respect to classification error probability.	Assumptions such as Normal and Cauchy distribution of the data and independency of features are often invalid.
LDA	Analytically simple, and computationally less extensive.	Regularization is often needed to hold the feature dimension below a certain level [128].
SVM	Globally optimal.	Algorithmic complexity is high. Unbalanced training may cause overriding minority class by majority class.

Table 3

CAD studies of nodules and nodular patterns.

Study	Features	Classifier	Data	Performance or ROC/FP rates	Ref.
Nodule characterization (malignant/benign)	Shape and intensity features	Rule based and Bayes	CT	Accuracy 97.1% FP: 17.6 per scan	[49]
Nodule Characterization (malignant/benign)	Surface features	LDA, SVM	CT	Accuracy 85.7%	[52]
Nodule Characterization (malignant/benign)	Co-occurrence matrix based features, shape and size features	ANN	CT	Sensitivity 90% A_z=0.79	[48]
Nodule Characterization and detection	LoG and Gabor Kernels	ANN	X-ray	95.7–98% FP:4–10 per scan	[13]
Nodule Characterization and detection	ROI, Volume, roundness, intensity, moments, and surface features	ANN	CT	Sensitivity 71–84% FP:4–10 per scan	[53]
Nodule Characterization and detection	Combination of contrast, histogram, and gradient features.	SVM	CT	Sensitivity 100% Specificity 56.4%	[54]
Detection of GGO Nodules	Shape features, volume, sphericity, compactness, and HU values	Rule Based and Bayes	CT	Accuracy 92.3% FP: 12.7 per scan	[51]

Table 4

CAD studies of interstitial lung disease.

Study	Features	Classifier	Data	Performance or ROC / FP rates	Ref.
Interstitial Lung Disease classification	First and second order statistics, wavelet and GLCM	SVM	CT	A_z : 0.831–0.968	[119]
Interstitial Lung Disease classification	Multi-scale filter- banks, moments, gradient of grey level features	LDA SVM	X-ray	A_z : 0.78	[86]
Interstitial Lung Disease classification	General purpose filter-banks	LDA SVM kNN	CT	A_z : 0.795	[120]
Interstitial Lung Disease classification (Emphysema, GGO, honeycomb,etc.)	Adaptive Multiple feature method including first order statistics and GLCM	Bayes SVM	CT	Sensitivity 83.25% Specificity 97.75% (for best cases)	[70]
Interstitial Lung Disease quantification (reticular, nodular, reticulonodular, etc.)	Multi-scale filter banks, shape features moments, energy and local texture features	kNN	X-ray	A_z : 0.97 improved from 0.948	[27,28] [40–45]
Interstitial Lung Disease classification (septal lines, honeycombs, etc.)	Local texture moments, size and energy features, homogeneity of textures, fineness and coarseness of textures	ANN	X-ray	A_z : 0.911 improved from 0.826	[15] [121,122]

Table 5

Summary of CAD studies for the characterization of other pulmonary conditions.

Study	Features	Classifier	Data	Performance	Ref.
Abnormality Classification	Statistical and fractal features, AMFM	Bayes	CT	Accuracy 51.7%	[59]
Abnormality Classification (GGO, reticular,nodular Emphysematous, etc.).	Grey-level distribution and geometric measures	ANN	CT	Sensitivity 88–100% Specificity 88.1%	[47]
Abnormality Classification	Moments, filter-banks, gradient features	kNN	CT	A_z : 0.74–0.95	[10]
Abnormality Classification	Lobular feature sets, Energy, size and GLCM	Decision Trees with Hash-table	CT	Avg.Accuracy 72%	[37]
Fibrosis Detection	Histogram statistics, GLCM and run-length features	SVM	CT	Accuracy 90%	[123]
Obstructive Lung Disease	Grey-level uniformity moments, GLCM	Bayes	CT	Sensitivity 74% Specificity 92%	[68]
GGO detection	Kohonen Feature maps	Multiple NN	CT	Sensitivity 99% Specificity 83%	[124]
Honeycomb detection	GLCM	Decision Trees Bayes	CT	Sensitivity 97.4% Specificity 85.5%	[69]
GGO Detection w/o nodules	Histogram features	Bayes	CT	Sensitivity 86% Specificity 96.5%	[76]
GGO Detection	Kurtosis, Surface, curvatures and grey level features	ANN	CT	A_z : 0.92 Sensitivity 94.3%	[55]